Applied Soft Computing 56 (2017) 317–330

Contents lists available at ScienceDirect

Applied Soft Computing

journal homepage: www.elsevier.com/locate/asoc

A neural network-based local rainfall prediction system using meteorological data on the Internet: A case study using data from the Japan Meteorological Agency

Tomoaki Kashiwao[a,b,*], Koichi Nakayama[a], Shin Ando[c], Kenji Ikeda[d], Moonyong Lee[e], Alireza Bahadori[b]

[a] Department of Electronics and Control Engineering, National Institute of Technology, Niihama College, 7-1 Yagumo-cho, Niihama, Ehime 792-8580, Japan
[b] School of Environment, Science and Engineering, Southern Cross University, P.O. Box 157, Lismore, NSW 2480, Australia
[c] Graduate School of Science and Engineering, Ehime University, 3, Bunkyo-cho, Matsuyama, Ehime 790-8577, Japan
[d] Graduate School of Institute of Technology and Science, Tokushima University, 2-1 Minamijosanjima-cho, Tokushima 770-8506, Japan
[e] School of Chemical Engineering, Yeungnam University, Dae-dong 214-1, Gyeongsan 712-749, Republic of Korea

ARTICLE INFO

Article history:
Received 8 August 2015
Received in revised form 9 February 2017
Accepted 3 March 2017
Available online 18 March 2017

Keywords:
Local rainfall prediction
Precipitation
Meteorological data
Neural networks
Big data

ABSTRACT

In this study, we develop and test a local rainfall (precipitation) prediction system based on artificial neural networks (ANNs). Our system can automatically obtain meteorological data used for rainfall prediction from the Internet. Meteorological data from equipment installed at a local point is also shared among users in our system. The final goal of the study was the practical use of "big data" on the Internet as well as the sharing of data among users for accurate rainfall prediction. We predicted local rainfall in regions of Japan using data from the Japan Meteorological Agency (JMA). As neural network (NN) models for the system, we used a multi-layer perceptron (MLP) with a hybrid algorithm composed of back-propagation (BP) and random optimization (RO) methods, and radial basis function network (RBFN) with a least squares method (LSM), and compared the prediction performance of the two models. Precipitation (total amount of rainfall above 0.5 mm between 12:00 and 24:00 JST (Japan standard time)) at Matsuyama, Sapporo, and Naha in 2012 was predicted by NNs using meteorological data for each city from 2011. The volume of precipitation was also predicted (total amount above 1.0 mm between 17:00 and 24:00 JST) at 16 points in Japan and compared with predictions by the JMA in order to verify the universality of the proposed system. The experimental results showed that precipitation in Japan can be predicted by the proposed method, and that the prediction performance of the MLP model was superior to that of the RBFN model for the rainfall prediction problem. However, the results were not better than those generated by the JMA. Finally, heavy rainfall (above 10 mm/h) in summer (Jun.–Sep.) afternoons (12:00–24:00 JST) in Tokyo in 2011 and 2012 was predicted using data for Tokyo between 2000 and 2010. The results showed that the volume of precipitation could be accurately predicted and the caching rate of heavy rainfall was high. This suggests that the proposed system can predict unexpected local heavy rainfalls as "guerrilla rainstorms."

1. Introduction

Accurate prediction of rainfall (precipitation) is challenging due to the complexity of meteorological phenomena. Rainfall is caused by a variety of meteorological conditions and the mathematical model for it is nonlinear. Numerical weather prediction systems run by the Japan Meteorological Agency (JMA) operate on supercomputers, and are based on the method used to simulate equations of meteorological phenomena using a mesoscale model and a local forecast model [1]. However, it is difficult for users in general to use supercomputers. At the same time, weather forecasting methods based on neural networks (NNs) [2–5], which are implemented on general-purpose computers, have been investigated intensively in recent years [6]. NNs can be applied for the identification of nonlinear systems in various fields of engineering (in particular, our research group has used NNs in petroleum engineer-

* Corresponding author at: Department of Electronics and Control Engineering, National Institute of Technology, Niihama College, 7-1 Yagumo-cho, Niihama, Ehime 792-8580, Japan.
E-mail address: kashiwao@ect.niihama-nct.ac.jp (T. Kashiwao).

http://dx.doi.org/10.1016/j.asoc.2017.03.015
1568-4946/

ing [7–15,10,16–18,16,19,20]), and can be used for meteorological prediction of rainfall [21–30], the direction of wind, its velocity [31], rainfall runoffs [32–36], and landslides [37]. However, past research on local rainfall (weather) prediction in Japan has only been performed in a limited number of areas and terms [23,25,31]. Therefore, in this paper, we develop a system to predict local rainfall (and other weather relevant to crop harvests, etc.) based on NNs [38]. In our system, arbitrary meteorological data can be automatically obtained from the Internet and used for rainfall prediction. Moreover, data from equipment installed at a local point is used for more accurate local rainfall prediction at each point. If meteorological data can be shared among users via the Internet, the accuracy of rainfall prediction can be enhanced. In first stage of the research, we verify the effectiveness of local rainfall prediction based on NNs using meteorological data obtained from the Internet in Japan. Practical use of "big data" on the Internet is an important subject of research that has a wide variety of applications [39,40]. Moreover, big data analysis based on NNs has been studied intensively in various fields in recent years [41,42]. If big data can be efficiently used in the proposed developed system, rainfall prediction can be rendered more accurate, and our system can hence be applied for the prediction of other meteorological phenomena in related areas of research due to its combination with NNs.

In recent years, urban areas in Japan have witnessed increasing amounts of unexpected local heavy rainfall at approximately 50–100 mm/h—called "guerrilla rainstorm"—due to the heat island phenomenon and global warming [43–46]. It is difficult to predict guerrilla rainstorms, which occur suddenly in summer afternoons. They cause floods and bring traffic to a standstill, which results in significant economical loss. The prediction of such rainfall is thus important for disaster prevention. In this study, mechanisms of rainfall in Japan and heavy summer afternoon rainfall in Tokyo are identified as NNs using meteorological data obtained from the Internet. Past and present meteorological data can be obtained from the website of the JMA [47]. Our previous paper reported on the prediction of heavy rainfall in summer afternoons in Tokyo as well as precipitation in Matsuyama, Sapporo, and Naha in order to the confirm effectiveness of our method based on only hitting numbers of precipitation day prediction [38]. In this study, the results were evaluated once again on the basis of an evaluation method developed by the JMA in order to investigate the accuracy of the method. Furthermore, precipitation at 16 observation points (cities) over Japan was predicted anew in order to verify both the accuracy and universality of the proposed system in Japan. The prediction results of the proposed method were compared with those of the JMA to evaluate the basic performance of our system with appropriate evaluation indices, and the prediction results of JMA could be fine target and index value for rainfall prediction experiments because JMA provides the most reliable weather forecast in Japan. (These results are not usually compared because the method and target of prediction of the JMA were different from those of ours method. JMA rainfall prediction based on physical simulations on a supercomputer is intended for a large area. By contrast, our prediction, which uses various kinds of data, is specialized to local prediction that cannot be covered by JMA prediction.)

In this paper, we compare the prediction performance of a multi-layer perceptron (MLP) NN with that of a radial bias function network (RBFN) [2–5]. An MLP model requires a considerable amount of computation time for training using the back-propagation (BP) learning method due to the local solution problem. Thus, hybrid algorithm composed of BP and the random optimization (RO) method was used to training the MLP [2]. Moreover, the hybrid algorithm was improved to reduce computation time. By contrast, the calculation of the RBFN was accomplished immediately by the least squares method (LSM). In past research, a three-layer perceptron (3LP, the most typical type of MLP) [23–26,29] and RBFN [21,30] were used for rainfall prediction. In general, RBFN is better than 3LP for prediction problems; however, the performance of 3LP is slightly better than that of RBFN for river-flow prediction [33] and landslide prediction [37], and the exact difference between 3LP and RBFN is inexact in the rainfall run-off prediction problem [35].

In Section 2, the proposed system and plans for future research are introduced. Section 3 is dedicated to a description of NN models and the training methods used. In Section 4, we explain the meteorological data used for experiments and the evaluation indices of the JMA, and reflect on the results of the prediction of rainfall in Matsuyama, Sapporo, and Naha in 2012 on the basis of the evaluation method of the JMA. Moreover, the results of our precipitation prediction at 16 points over Japan were compared with the JMA's results. In Section 5, the prediction results of heavy rainfall in the summer in Tokyo in 2011 and 2012 are detailed. Finally, we offer our conclusions in Section 6.

2. Proposed system

The proposed system aims at using data on the Internet as "big data" for rainfall prediction (Fig. 1). If efficient meteorological data can be obtained from the Internet and shared among users, rainfall prediction can be made more accurate. One of the most efficient types of data for rainfall prediction in Japan is past meteorological data from the Japan Meteorological Agency (JMA) [47]. In first step of our research, data from the JMA was used for rainfall prediction.

The proposed system could automatically obtain meteorological data from the JMA website. We could easily change the conditions for meteorological data (date, time, and observation point) via the graphical user interface of our system (Fig. 2), developed in Microsoft Visual C# 2010. Moreover, the training of the NNs as well as rainfall prediction was accomplished without complicated operations. In the next step, data from equipment installed at a local point was used for rainfall prediction at each point. Meteorological data at our college (National Institute of Technology (NIT), Niihama college, Ehime, Japan) is now being collected by using a meteorological data logger.

The use of big data on the Internet must be effective and efficient for rainfall prediction in terms of prediction accuracy and convenience of collecting data. However, choosing an appropriate selection method for data is a challenging problem because there are massive amounts of relevant data on the Internet. NNs have been used for the analysis and sorting of big data. In particular, "deep-learning" technology based on NNs is one of the most effective methods to this end [48]. In this study, we need to collect data related to precipitation in each local spot that we analyzed from the Internet. However, if the data items are too numerous, NN training and computation become difficult and time-consuming. Therefore, an appropriate number of data items that can ensure prediction accuracy must be selected from the collected data. In the final stage of the study, we will use deep-learning technology to collect and select big data on the Internet for rainfall prediction based on the proposed method. (The kinds of effective meteorology data are different for each local area due to differences in meteorological conditions, such as a location and topography. Thus, the selection of suitable data for each local spot is an important factor for local rainfall prediction.)

3. Neural networks

In this section, we explain and compare the NN models used for our rainfall prediction experiment. General NN models—namely, a multi-layer perceptron (MLP) and a radial basis function network (RBFN)—were used for rainfall modeling. A three-layer perceptron

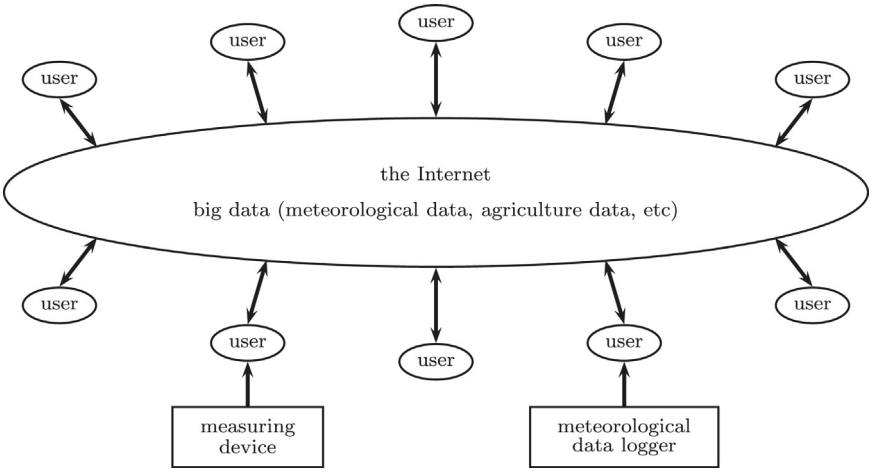

Fig. 1. The developed system.

(3LP) was chosen as the most typical MLP in this study. A hybrid algorithm composed of back-propagation (BP) and random optimization (RO) methods [2] was used to train the 3LP model. The BP method is based on the steepest descent method, and encounters a local solution problem. Its training is thus time consuming; however, the hybrid algorithm can solve these problems. The RO method enables the results of training to avoid the local solution problem. On the contrary, the RBFN has the advantage of short computation time over the 3LP because optimized weights therein can be obtained by the least squares method (LSM). Moreover, in spite of the same training data, there is a difference in training results between 3LP and RBFN. Especially in the case of 3LP, the results are different for each instance of training. Conversely, the RBFN has the characteristic whereby a result is uniquely determined by LSM given the same parameters.

3.1. Three-layer perceptron (3LP)

In this study, we used the sigmoid function as the output function of the units of the 3LP (Fig. 3). (Ref. [23] shows the best results of rainfall prediction using a combination of a three-layer hybrid structure and the sigmoid function.) The 3LP is composed of three layers: an input layer, a hidden layer, and an output layer. N, M, and L are the numbers of units of the input layer, the hidden layer, and the output layer, respectively ($L = 1$ in this study). When patterns of a teaching signal are defined as $p = 1, \ldots, P$ (P is the number of

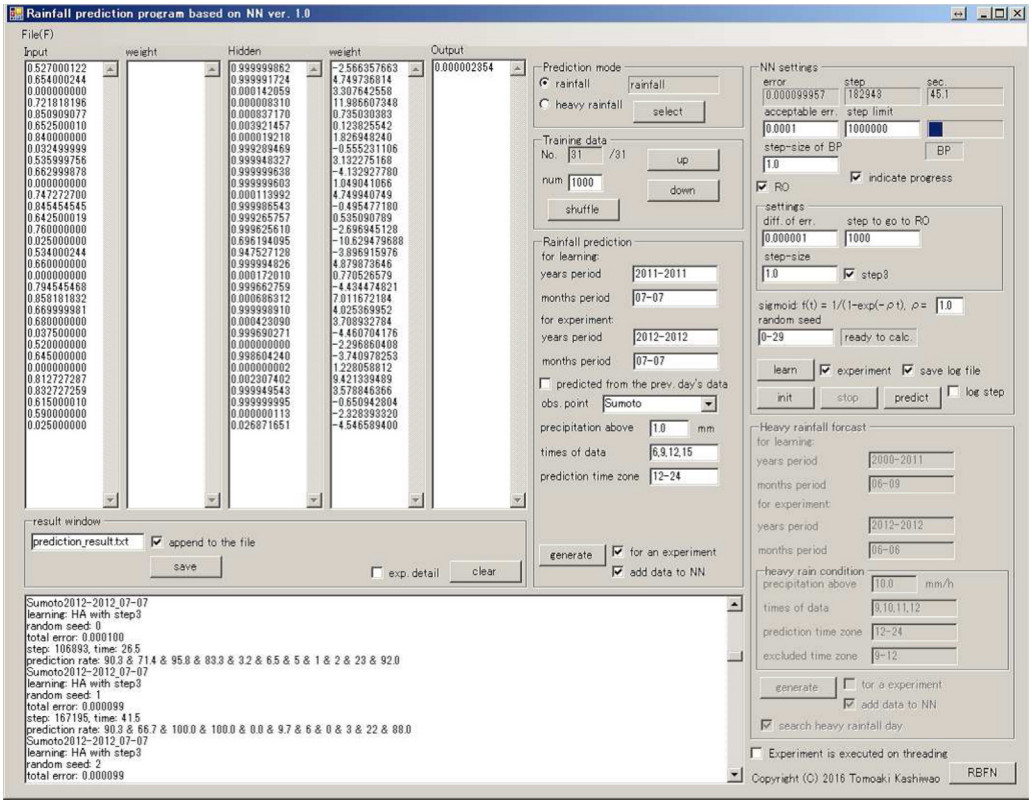

Fig. 2. User interface of the developed system.

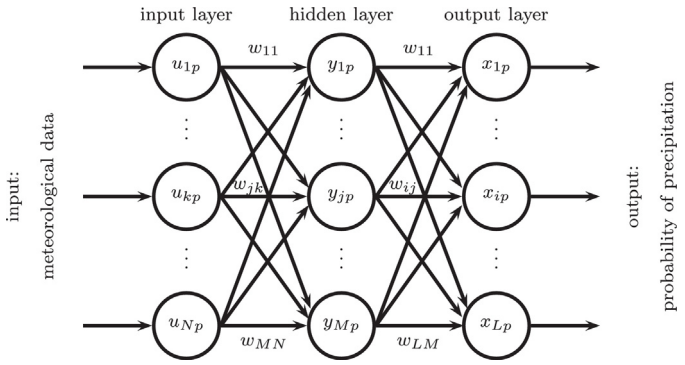

Fig. 3. Three-layer perceptron.

patterns), the output of the ith unit of the output layer for the pth pattern is defined as

$$x_{ip} = h(z_{ip}), \tag{1}$$

$$z_{ip} = \sum_j w_{ij} y_{jp}, \tag{2}$$

where y_{jp} is an output of the jth unit of the hidden layer for the pth pattern, and w_{ij} is the weight from the jth unit of the hidden layer to the ith unit of the output layer. $h(\cdot)$ is the sigmoid function:

$$h(t) = \frac{1}{1+\exp(-\beta t)}, \quad \beta > 0, \tag{3}$$

where β is the parameter of the slope of the function ($\beta = 1.0$ in this study). The output of the jth unit of the hidden layer for the pth pattern is defined as

$$y_{jp} = h(z_{jp}), \tag{4}$$

$$z_{jp} = \sum_j w_{jk} u_{kp}, \tag{5}$$

where w_{jk} is the weight from the kth unit of the input layer to the jth unit of the hidden layer, and u_{kp} is the input signal from the pth pattern to the kth unit of the input layer.

In general, the number of units of the hidden layer affects prediction accuracy: if it is set larger, the approximation performance of the 3LP for an objective is rendered more accurate; however, the computation time required for training becomes longer, and its convergence is hence worsened. As a result of the verification of computation time and the convergence of training, it was determined as $M = N$ in this study.

3.2. Back-propagation (BP) method

The BP method is the typical training method employed to optimize the weight of NNs using the steepest descent method. The total error function $E_s(\boldsymbol{w})$ at training step s for all patterns of teaching signals is defined as follows:

$$E_s(\boldsymbol{w}) = \sum_p E_p(\boldsymbol{w}), \tag{6}$$

$$E_p(\boldsymbol{w}) = \frac{1}{2}\sum_i (\bar{x}_{ip} - d_{ip})^2, \tag{7}$$

where d_{ip} is an output of the pth pattern of the teaching signal, $\bar{x}_{ip}$ is that of the ith unit of the output layer for the pth pattern, and $E_p(\boldsymbol{w})$ is an error function for the pth pattern. Weight vector $\boldsymbol{w}$, composed of weights w_{ij} and w_{jk}, is updated using the steepest descent method, and is subject to the minimization of the total error function $E_s(\boldsymbol{w})$. Updates of w_{ij} and w_{jk} are given by

$$w_{ij} = w_{ij} + \mu_{BP}\delta_{ip} y_{jp}, \tag{8}$$

$$\delta_{ip} = -(\bar{x}_{ip} - d_{ip}) h'(z_{ip}), \tag{9}$$

$$w_{jk} = w_{jk} + \mu_{BP}\delta_{kp} u_{kp}, \tag{10}$$

$$\delta_{kp} = h'(z_{kp}) \sum_j \delta_{jp} w_{jk}, \tag{11}$$

respectively, where μ_{BP} is step size. Thus, as these calculations are repeated in each step, the weights are optimized for the teaching signals.

3.3. Random optimization (RO) method

The RO method is a training method for weights that uses random numbers. In this study, weights are updated by the calculation below:

$$w_{ij} = w_{ij} + \mu_{RO} v_{ij}, \tag{12}$$

$$w_{jk} = w_{jk} + \mu_{RO} v_{jk}, \tag{13}$$

where v_{ij} and v_{jk} are normal random numbers according to $N(0, 1)$ and μ_{RO} is step size. When the value of the total error function $E_s(\boldsymbol{w})$ following calculation is compared with that prior to the calculation $E_{s-1}(\boldsymbol{w})$ at each step, weights w_{ij} and w_{jk} are updated as values following calculation if $E_s(\boldsymbol{w}) < E_{s-1}(\boldsymbol{w})$, and are not updated if $E_s(\boldsymbol{w}) \geq E_{s-1}(\boldsymbol{w})$.

3.4. Hybrid algorithm

The BP method encounters the local solution problem, whereby the total error function $E_s(\boldsymbol{w})$ falls into a local minimum. On the contrary, the RO method has sufficiently satisfactory characteristics to find a global minimum in a compact set. Thus, a hybrid algorithm composed of the BP and RO methods [2] is used in this study. Furthermore, its transition condition from BP to RO is contrived to shorten learning time. The improved hybrid algorithm is as follows:

Hybrid algorithm

- Set step numbers as $s = 0$, $n = 0$, and initialize w_{ij}, w_{jk} as random numbers within proper range.
- Set $s = s + 1$, and update weights w_{ij} and w_{jk} using BP; calculate the value of the total error function $E_s(\boldsymbol{w})$. If $E_s(\boldsymbol{w}) \leq E_a$, end the training. If $|E_s(\boldsymbol{w}) - E_{s-1}(\boldsymbol{w})| < E_{RO}$, go to Step 3; else, set $n = 0$, and repeat Step 2.
- Set $n = n + 1$, and if $n = S_{RO}$, go to Step 4; else go to Step 2.
- Set $s = s + 1$, and calculate w_{ij}, w_{jk}, and $E_s(\boldsymbol{w})$ with the RO method. If $E_s(\boldsymbol{w}) \leq E_a$, end the training. If $E_s(\boldsymbol{w}) < E_{s-1}(\boldsymbol{w})$, go to Step 2; else, restore w_{ij} and w_{jk} to the values of the previous step $s-1$, and repeat Step 4.

E_a is an acceptable error as the condition to finish training, E_{RO} represents the condition of difference between the total error function $E_{s-1}(\boldsymbol{w})$ and the $E_s(\boldsymbol{w})$ steps in order to set $n = n + 1$, where n is the number of the step required to satisfy the condition, and S_{RO} is the condition where n moves on to the RO method from the BP method. The value of the total error function is first reduced as much as possible using the BP method, following which the RO method is used when it falls into a local minimum. The training then returns to the BP method after escaping from the local minimum through the RO method. By repeating these steps, the solution converges to a global minimum.

Fig. 4 shows a comparison of training efficiency between the BP method and the hybrid algorithm. When experiments began with

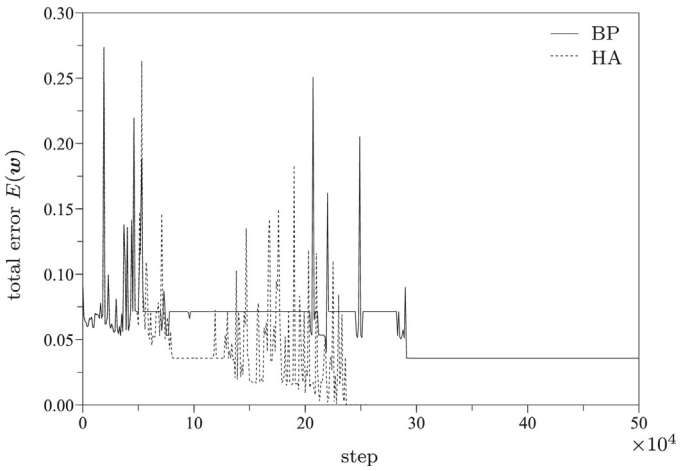

Fig. 4. Transition of the number of steps in the BP method and the hybrid algorithm (HA), which were plotted for 1000 steps (input layer: 32; hidden layer: 32; output layer: 1; training data: 28).

the same initial parameters, the total error of the hybrid algorithm converged to a smaller value than that of the BP method. The training parameters were set as $\mu_{BP} = 1.0$, $\mu_{RO} = 1.0$, $E_a = 10^{-4}$, $E_r = 10^{-6}$, and $S_{RO} = 1000$. In case training could not converge, it ended when the number of steps reached $s = 10^6$ in experiments described in Sections 4.3 and 5, and $s = 5 \times 10^5$ for the experiment in Section 4.4.

When the RO method was implemented on a program, the training time was longer than that of the BP method, depending on programming language and execution environment, because all weights needed to be saved temporally when these weights were updated. Therefore, we added Step 3 in order to judge when to move on to the RO method from the conventional hybrid algorithm [2]. If the training moved on to the RO method when $|E_{s+1}(\boldsymbol{w}) - E_s(\boldsymbol{w})| < E_r$ in the Step 2 directory, the number of steps of the RO method increased, so that Step 3 had a function to adjust its frequency to move on to the RO method. In case the number of units was larger, the computation time required for training could be reduced if step size μ_{BP} was set as the larger value and Step 3 was added. Fig. 5 shows the graph of the relationship between the steps and the computation time when training concluded with Step 3 and without Step 3 under the execution conditions (Table 1). The experiments with and without Step 3 began with the same initial parameters,

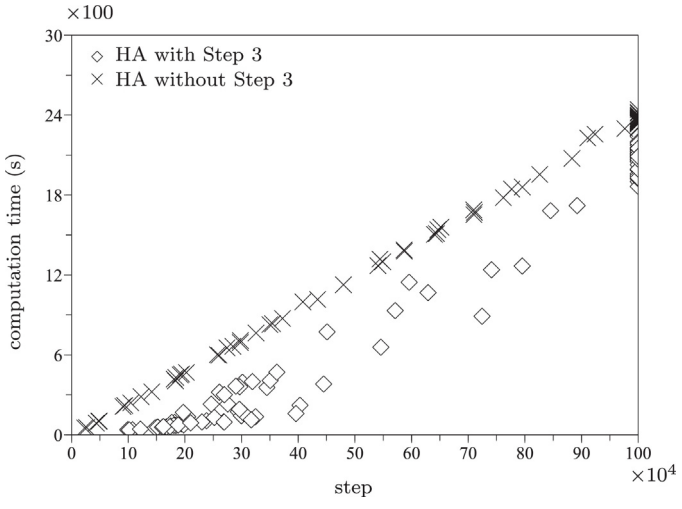

Fig. 5. Computation time of the hybrid algorithm (HA) with Step 3 and without Step 3 (input layer: 32; hidden layer: 32; output layer: 1; training data: 28).

Table 1
Execution environment.

OS	Windows 7 Professional 64 bit
IDE	Visual C# 2010 (Microsoft Visual Studio 2010)
CPU	Intel Core i7-3770 3.4 GHz
RAM	16 GB

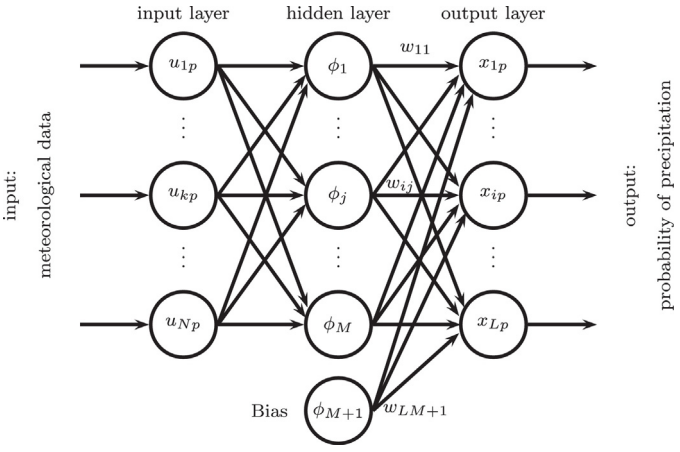

Fig. 6. RBF network.

and the results of 100 iterations were plotted for each (The averages of computation times, Step 3: 1001 s; without Step 3: 1692 s).

3.5. Radial basis function network (RBFN)

RBFN is used to approximate a nonlinear function and rainfall prediction as well as MLP in [21]. The network structure of RBFN is similar to that of 3LP (Fig. 6). However, a Gaussian function

$$\phi_j(U_p) = \exp\left(-\frac{\|U_p - \bar{U}_j\|_2}{2\sigma^2}\right) \quad \text{for } j = 1, \ldots, M, \tag{14}$$

$$\phi_{M+1}(U_p) = 1, \tag{15}$$

$$(U_p)_k = u_{kp}, \tag{16}$$

$$(\bar{U}_j) = [\bar{u}_j, \ldots, \bar{u}_j]^\top, \tag{17}$$

is used as the output function for the units instead of the sigmoid function (Eq. (3)). $U_p \in R^N$ and $\bar{U} \in R^N$ are an output vector and a center vector for the pth input pattern, respectively, $\bar{u}_j \in R$ is the value of the center of the Gaussian function, which is allocated to each unit of the hidden layer, $\sigma \in R$ is the standard deviation, $\phi_{M+1}(U_p)$ is a bias, and u_{kp} is an input signal for the kth unit of the input layer for the pth input pattern.

From the output and weights of each unit of the hidden layer, the output of each unit of the output layer is represented as

$$x_{ip} = \sum_{j=1}^{M+1} w_{ij}\phi_j(U_p). \tag{18}$$

If the center $\bar{u}_j$ and standard deviation σ are determined, the best approximation of the weight vector can be obtained by LSM at the same time:

$$W^\top = \Phi^+ X, \tag{19}$$

$$\Phi^+ = (\Phi^\top \Phi)^{-1}\Phi^\top, \tag{20}$$

$$(W) = (w_{ij}), \tag{21}$$

$$(\Phi)_{pj} = \phi_j(U_p), \tag{22}$$

$$(X)_{pi} = d_{ip}, \tag{23}$$

Table 2
Meteorological data and their normalization.

Signal	Kinds of data	Value range	Normalized value range
Input	Atmospheric pressure (on-site)	940–1040 hPa	0–1
	Atmospheric pressure (sea-level)	940–1040 hPa	0–1
	Precipitation	Above 0.5 mm/h	1
		Otherwise	0
	Temperature	−15 to 40 °C	0–1
	Open-air temperature	−25 to 30 °C	0–1
	Vapor pressure	0–40 hPa	0–1
	Humidity	0–100%	0–1
	Wind velocity	0–40 m/s	0–1
Output	Total precipitation	Above 0.5 (or 1.0) mm	1
		Otherwise	0

where Φ^+ is a pseudo-inverse matrix. Therefore, the number of calculations involved in RBFN is much smaller than those in 3LP, which is trained using the steepest descent method. Using the numerical calculation software Scilab (Scilab Enterprises, France), we can obtain the optimized result within 1 s under the execution environment (Table 1). In this study, the center of the Gaussian function of each unit of the hidden layer is given by

$$\bar{u}_j = \frac{j-1}{M-1} \quad \text{for } j = 1, \ldots, M, \tag{24}$$

at the same range between 0–1 as the range of output. In this case, the standard deviation σ of the Gaussian function of each unit of the hidden layer can be set the same value, and the expression performance of a nonlinear function of RBFN depends on σ. The best value of σ is found while changing the value as follows:

$$\sigma = \frac{1}{M-1} + 0.01l \quad \text{for } l = 0, 1, \ldots, 100. \tag{25}$$

It is given by the value between the centers of the Gaussian function because the accuracy of the approximation function worsens if σ is too small. The number of units of the hidden layer is set as $M = N$ for the comparison of prediction performance between 3LP and RBFN.

4. Rainfall prediction

In this section, we explain the meteorological data used for rainfall prediction as well as the evaluation method of the JMA. The prediction experiments for Sapporo, Naha, Matsuyama, and 16 points (cities) of all parts of Japan are detailed, the effectiveness of the proposed method is verified, and a comparison of the prediction performance between 3LP and RBFN is described. Moreover, the prediction results are compared with those of the JMA.

4.1. Meteorological data

The website of the Japan Meteorological Agency (JMA) provides meteorological data from 1976 to the present every 10 minutes at many points across the country [47]. In this study, the proposed system automatically collected eight types of meteorological data: atmospheric pressure (on site and sea level), amount of precipitation, (air and open-air) temperature, vapor pressure, humidity, and wind velocity. These data were normalized as in Table 2 for the input signal of the NNs, and wind direction (Table 3) was added to the input signal for the experiments described in Section 5. The total amount of precipitation was normalized as "1 when above 0.5 mm" and "0 when below 0.5 mm" for the output signal in Section 4.3. In general, the probability of precipitation was based on precipitation above 1.0 mm of the total amount. However, if precipitation of 0.5 mm above the total amount was targeted, the number of days witnessing precipitation could be increased and the efficiency of the training of NNs enhanced. In Section 4.4, in order to compare experimental results with those of the JMA, the objective was determined to be the total precipitation above 1.0 mm. Moreover, if there was a deficit in the data for a given day, the day was removed from the training and prediction experiments.

In Section 4, monthly data from 2011 and 2012 are used to train NNs and test them (experiments), respectively. In Section 5, data for the summer of 2000–2010 and 2011–2012 are used for the training of the NNs and the experiments, respectively. A number of the training and experimental data were different because erroneous data were removed.

4.2. Evaluation index

For the JMA, the prediction results were verified by the following evaluation indices [49]:

$$\text{Total hit rate: } THR = \frac{A+D}{N} \times 100 \ (\%), \tag{26}$$

$$\text{Hit rate of precipitation: } HRP = \frac{A}{A+C} \times 100 \ (\%), \tag{27}$$

$$\text{Hit rate of non-precipitation: } HRN = \frac{D}{B+D} \times 100 \ (\%), \tag{28}$$

$$\text{Caching rate: } CR = \frac{A}{A+B} \times 100 \ (\%), \tag{29}$$

$$\text{Overlooking rate: } OR = \frac{B}{N} \times 100 \ (\%), \tag{30}$$

$$\text{Swing-and-miss rate: } SMR = \frac{C}{N} \times 100 \ (\%), \tag{31}$$

where the number of events A, B, C, and D were defined by the confusion matrix in Table 4, and a population was defined as $N = A + B + C + D$. A is a number of events where the prediction hit the precipitation (when the result of observation was precipitation), B is the number of events where the prediction missed precipitation (when the result of observation was non-precipitation), C is the number of events where the prediction missed non-precipitation (when the result of observation was precipitation), and D is the number of events where the prediction hit non-precipitation (when the result of observation was non-precipitation). "Observation"

Table 3
Normalization of wind direction.

Wind direction	Normalized value	Wind direction	Normalized value
N	0.0625	S	0.5625
NNE	0.125	SSW	0.625
NE	0.1875	SW	0.6875
ENE	0.25	WSW	0.75
E	0.3125	W	0.8125
ESE	0.375	WNW	0.875
SE	0.4375	NW	0.9375
SSE	0.5	NNW	1
None	0		

Table 4
Confusion matrix of JMA.

	Prediction	
	Precipitation	Non-precipitation
Observation		
Precipitation	A	B
Non-precipitation	C	D

here means observed real weather. The higher the values of *THR*, *HRP*, *HRN*, and *CR*, the better the prediction result. Contrarily, the higher the values of *OR* and *SMR*, the worse the prediction result. *CR* is the most important value from the point of view of disaster prevention; however, the prediction becomes a case of "the boy who cried wolf" (whereby there exist many cases where the precipitation expected according to the prediction did not occur) if *HRP* was too low.

4.3. Sapporo, Matsuyama, and Naha

The precipitation (total amount above 0.5 mm) in Sapporo, Matsuyama, and Naha in 2012 was predicted by NNs trained with data for the respective cities from 2011. In order to verify the effectiveness of the proposed method, Sapporo (the biggest city of Hokkaido in the northern-most region of Japan), Matsuyama (the largest city in Shikoku), and Naha (the southern-most big city in Japan) were chosen (Fig. 7). The data in Table 2 at 3:00, 6:00, 9:00, and 12:00 JST (Japan standard time: UTC+9) was set as the input signal (total number: 32), and the output signal of the teaching signal was given by the total amount of precipitation in the afternoon (12:00–24:00 JST). Precipitation for each day of each month at each city in 2012 was predicted by NNs trained using data from the corresponding month in 2011. The object precipitation was above 0.5 mm of the total amount. Thus, the prediction result was defined as "precipitation" if the total amount was above 0.5 mm, and as "non-precipitation" if the total amount was below 0.5 mm. A prediction result was defined as "the precipitation when the output of NNs ≥0.5" and "non-precipitation when the output of NNs <0.5." In the experiments, 30 of the 3LP NNs were trained while changing each of the initial weights, and 101 of the RBFN NNs were trained while changing the standard deviation, as in Eq. (25).

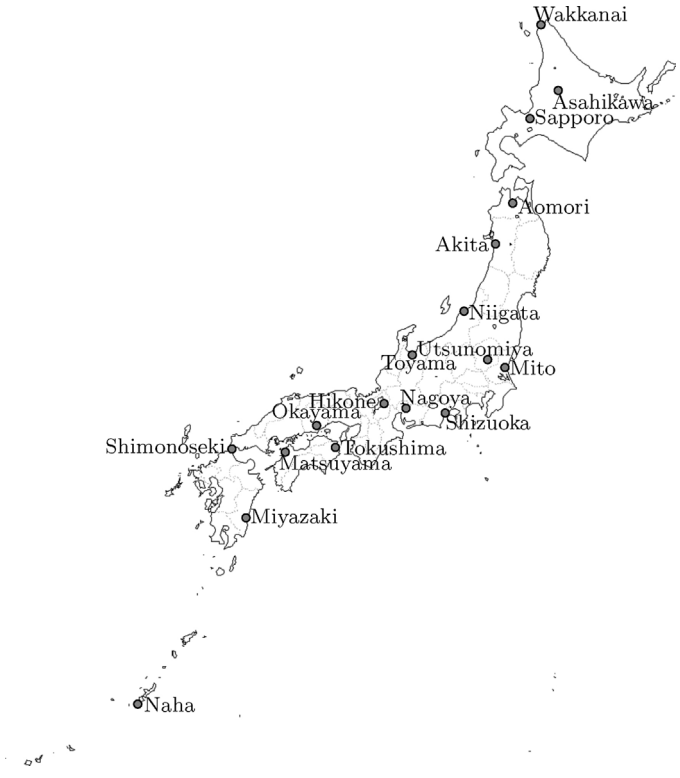

Fig. 7. Observation points in Japan (the map image from CraftMAP [50]).

Tables 5–10 show the experimental results for Sapporo, Matsuyama, and Naha. Result 1 shows the best prediction results for a number of *A* events, and result 2 represents the best prediction results for a number of *D* events (if result 1 included the best result of *D*, result 2 was the second-best result of *A* or *D*.) Moreover, results biased toward precipitation or non-precipitation were removed. JMA in tables means the monthly average of the evaluation indices in the JMA's precipitation prediction for each area, including each city, which is listed on the organization's website [49]. The object of the prediction was precipitation between 17:00 and 24:00 JST each day, and was announced at 17:00 JST every day. The JMA's results are shown as a reference value of the prediction rate. Table 11 shows the total result for a year for each city.

The results for 3LP were better than those for RBFN in the experiments in general. However, there were months where the prediction results for RBFN were better than those for 3LP. Furthermore, we observed that there were relationships involving trade-offs between the number of *A* and *D* events. The larger the number of events of type *A*, the smaller those of type *D*. On the contrary, the larger the number of *D* events, the smaller that of *A* events. Moreover, *HRP* was low when *A* was large because the NNs of large *A* events tended to predict "precipitation" rather than "non-precipitation;" however, this implied the "the boy who cried wolf" results. Contrarily, the larger the number of *D* events, the higher *HRP* was, and the lower *CR* was. Therefore, the NNs for large number of *A* events needed to be chosen from the point of view of disaster prevention. Furthermore, the results were not considerably worse than those of the JMA (however, it was not easy to compare the results due to differences in conditions, such as time zone and size of object area).

4.4. 16 points in Japan

Precipitation for 16 points (cities) shown below in all regions of Japan was predicted in order to verify the accuracy of the method for the country.

- Wakkanai and Asahikawa in Hokkaido
- Aomori and Akita in Tohoku
- Mito and Utsunomiya in Kanto
- Sizuoka and Nagoya in Tokai
- Niigata and Toyama in Hokuriku
- Hikone in Kinki
- Tokushima in Shikoku
- Okayama and Shimonoseki in Chugoku
- Miyazaki in Kyushu
- Naha in Okinawa

For more accurate comparison with the JMA results, the conditions for the training data and the time zone of objective precipitation were changed: the input signals for the teaching signals were set as data at 6:00, 9:00, 12:00, and 15:00 JST (total number: 32), and the output signals of the teaching signals were given by the total amount of precipitation in the afternoon (17:00–24:00 JST). The object was changed to precipitation above 1.0 mm of the total amount because JMA's prediction targeted the total precipitation above 1.0 mm. In the experiments, 20 of the 3LP NNs were trained while changing the initial weights, and the condition for training step to end the training of 3LP was changed to $s = 5 \times 10^5$ from $s = 10^6$ in order to reduce the time needed for train-

Table 5
Prediction results for Sapporo in Jan.–Jun. 2012 (JMA: Ishikari).

Month	Model	Result	Evaluation index (%)						A number of events			
			THR	*HRP*	*HRN*	*CR*	*OR*	*SMR*	*A*	*B*	*C*	*D*
Jan.	3LP	Result 1	77.4	68.4	91.7	92.9	3.2	19.4	13	1	6	11
		Result 2	80.6	75.0	86.7	85.7	6.5	12.9	12	2	4	13
	RBFN	Result 1	54.8	50.0	71.4	85.7	6.5	38.7	12	2	12	5
		Result 2	58.1	66.7	57.1	14.3	38.7	3.2	2	12	1	16
	JMA	–	67.0	50.0	79.0	63.0	12.0	21.0	–	–	–	–
Feb.	3LP	Result 1	69.0	58.8	83.3	83.3	6.9	24.1	10	2	7	10
		Result 2	72.4	75.0	71.4	50.0	20.7	6.9	6	6	2	15
	RBFN	Result 1	69.0	63.6	72.2	58.3	17.2	13.8	7	5	4	13
		Result 2	65.5	58.3	70.6	58.3	17.2	17.2	7	5	5	12
	JMA	–	75.0	56.0	89.0	78.0	6.0	18.0	–	–	–	–
Mar.	3LP	Result 1	80.6	71.4	88.2	83.3	6.5	12.9	10	2	4	15
		Result 2	80.6	80.0	81.0	66.7	12.9	6.5	8	4	2	17
	RBFN	Result 1	54.8	43.8	66.7	58.3	16.1	29.0	7	5	9	10
		Result 2	58.1	33.3	60.7	8.3	35.5	6.5	1	11	2	17
	JMA	–	82.0	45.0	97.0	84.0	2.0	16.0	–	–	–	–
Apr.	3LP	Result 1	83.3	57.1	91.3	66.7	6.7	10.0	4	2	3	21
		Result 2	80.0	50.0	87.5	50.0	10.0	10.0	3	3	3	21
	RBFN	Result 1	73.3	37.5	86.4	50.0	10.0	16.7	3	3	5	19
		Result 2	80.0	50.0	84.6	33.3	13.3	6.7	2	4	2	22
	JMA	–	87.0	53.0	95.0	73.0	4.0	9.0	–	–	–	–
May	3LP	Result 1	80.6	53.8	100.0	100.0	0.0	19.4	7	0	6	18
		Result 2	77.4	50.0	90.5	71.4	6.5	16.1	5	2	5	19
	RBFN	Result 1	54.8	33.3	100.0	100.0	0.0	45.2	7	0	14	10
		Result 2	74.2	33.3	78.6	14.3	19.4	6.5	1	6	2	22
	JMA	–	92.0	65.0	98.0	90.0	1.0	7.0	–	–	–	–
Jun.	3LP	Result 1	96.7	100.0	96.2	80.0	3.3	0.0	4	1	0	25
		Result 2	93.3	100.0	92.6	60.0	6.7	0.0	3	2	0	25
	RBFN	Result 1	80.0	44.4	95.2	80.0	3.3	16.7	4	1	5	20
		Result 2	83.3	50.0	88.5	40.0	10.0	6.7	2	3	2	23
	JMA	–	90.0	17.0	98.0	46.0	2.0	8.0	–	–	–	–

Table 6
Prediction results for Sapporo in Jul.–Dec. 2012 (JMA: Ishikari).

Month	Model	Result	Evaluation index (%)						A number of events			
			THR	*HRP*	*HRN*	*CR*	*OR*	*SMR*	*A*	*B*	*C*	*D*
Jul.	3LP	Result 1	54.8	23.5	92.9	80.0	3.2	41.9	4	1	13	13
		Result 2	80.6	40.0	88.5	40.0	9.7	9.7	2	3	3	23
	RBFN	Result 1	54.8	23.5	92.9	80.0	3.2	41.9	4	1	13	13
		Result 2	74.2	28.6	87.5	40.0	9.7	16.1	2	3	5	21
	JMA	–	90.0	42.0	97.0	69.0	2.0	8.0	–	–	–	–
Aug.	3LP	Result 1	87.1	60.0	92.3	60.0	6.5	6.5	3	2	2	24
		Result 2	87.1	66.7	89.3	40.0	9.7	3.2	2	3	1	25
	RBFN	Result 1	67.7	27.3	90.0	60.0	6.5	25.8	3	2	8	18
		Result 2	71.0	25.0	87.0	40.0	9.7	19.4	2	3	6	20
	JMA	–	88.0	48.0	96.0	67.0	4.0	8.0	–	–	–	–
Sep.	3LP	Result 1	76.7	36.4	100.0	100.0	0.0	23.3	4	0	7	19
		Result 2	86.7	50.0	95.8	75.0	3.3	10.0	3	1	3	23
	RBFN	Result 1	40.0	18.2	100.0	100.0	0.0	60.0	4	0	18	8
		Result 2	83.3	33.3	88.9	25.0	10.0	6.7	1	3	2	24
	JMA	–	83.0	49.0	95.0	80.0	3.0	14.0	–	–	–	–
Oct.	3LP	Result 1	71.0	63.6	75.0	58.3	16.1	12.9	7	5	4	15
		Result 2	71.0	71.4	70.8	41.7	22.6	6.5	5	7	2	17
	RBFN	Result 1	71.0	63.6	75.0	58.3	16.1	12.9	7	5	4	15
		Result 2	64.5	60.0	65.4	25.0	29.0	6.5	3	9	2	17
	JMA	–	79.0	53.0	88.0	61.0	9.0	12.0	–	–	–	–
Nov.	3LP	Result 1	73.3	70.8	83.3	94.4	3.3	23.3	17	1	7	5
		Result 2	80.0	92.9	68.8	72.2	16.7	3.3	13	5	1	11
	RBFN	Result 1	70.0	90.9	57.9	55.6	26.7	3.3	10	8	1	11
		Result 2	53.3	100.0	46.2	22.2	46.7	0.0	4	14	0	12
	JMA	–	75.0	64.0	89.0	88.0	5.0	21.0	–	–	–	–
Dec.	3LP	Result 1	71.0	85.0	45.5	73.9	19.4	9.7	17	6	3	5
		Result 2	71.0	93.8	46.7	65.2	25.8	3.2	15	8	1	7
	RBFN	Result 1	61.3	82.4	35.7	60.9	29.0	9.7	14	9	3	5
		Result 2	54.8	100.0	36.4	39.1	45.2	0.0	9	14	0	8
	JMA	–	58.0	48.0	81.0	84.0	6.0	35.0	–	–	–	–

Table 7
Prediction results for Matsuyama in Jan.–Jun. 2012 (JMA: Chuyo).

Month	Model	Result	Evaluation index (%)						A number of events			
			THR	*HRP*	*HRN*	*CR*	*OR*	*SMR*	*A*	*B*	*C*	*D*
Jan.	3LP	Result 1	100.0	100.0	100.0	100.0	0.0	0.0	5	0	0	25
		Result 2	96.7	100.0	96.2	80.0	3.3	0.0	4	1	0	25
	RBFN	Result 1	90.0	66.7	95.8	80.0	3.3	6.7	4	1	2	23
		Result 2	90.0	75.0	92.3	60.0	6.7	3.3	3	2	1	24
	JMA	–	95.0	67.0	98.0	77.0	2.0	3.0	–	–	–	–
Feb.	3LP	Result 1	69.0	50.0	82.4	66.7	10.3	20.7	6	3	6	14
		Result 2	72.4	100.0	71.4	11.1	27.6	0.0	1	8	0	20
	RBFN	Result 1	82.8	75.0	85.7	66.7	10.3	6.9	6	3	2	18
		Result 2	69.0	50.0	70.4	11.1	27.6	3.4	1	8	1	19
	JMA	–	82.0	58.0	95.0	85.0	3.0	14.0	–	–	–	–
Mar.	3LP	Result 1	83.3	75.0	84.6	42.9	13.3	3.3	3	4	1	22
		Result 2	83.3	100.0	82.1	28.6	16.7	0.0	2	5	0	23
	RBFN	Result 1	63.3	35.7	87.5	71.4	6.7	30.0	5	2	9	14
		Result 2	80.0	60.0	84.0	42.9	13.3	6.7	3	4	2	21
	JMA	–	96.0	87.0	98.0	93.0	1.0	3.0	–	–	–	–
Apr.	3LP	Result 1	73.3	60.0	80.0	60.0	13.3	13.3	6	4	4	16
		Result 2	76.7	100.0	74.1	30.0	23.3	0.0	3	7	0	20
	RBFN	Result 1	60.0	40.0	70.0	40.0	20.0	20.0	4	6	6	14
		Result 2	70.0	100.0	69.0	10.0	30.0	0.0	1	9	0	20
	JMA	–	86.0	56.0	92.0	58.0	7.0	7.0 –	–	–	–	
May	3LP	Result 1	90.3	66.7	96.0	80.0	3.2	6.5	4	1	2	24
		Result 2	87.1	57.1	95.8	80.0	3.2	9.7	4	1	3	23
	RBFN	Result 1	83.9	50.0	95.7	80.0	3.2	12.9	4	1	4	22
		Result 2	90.3	75.0	92.6	60.0	6.5	3.2	3	2	1	25
	JMA	–	98.0	90.0	99.0	82.0	1.0	1.0 –	–	–	–	
Jun.	3LP	Result 1	83.3	83.3	83.3	76.9	10.0	6.7	10	3	2	15
		Result 2	83.3	90.0	80.0	69.2	13.3	3.3	9	4	1	16
	RBFN	Result 1	76.7	87.5	72.7	53.8	20.0	3.3	7	6	1	16
		Result 2	73.3	100.0	68.0	38.5	26.7	0.0	5	8	0	17
	JMA	–	89.0	76.0	94.0	85.0	4.0	7.0 –	–	–	–	

Table 8
Prediction results for Matsuyama in Jul.–Dec. 2012 (JMA: Chuyo).

Month	Model	Result	Evaluation index (%)						A number of events			
			THR	*HRP*	*HRN*	*CR*	*OR*	*SMR*	*A*	*B*	*C*	*D*
Jul.	3LP	Result 1	83.9	66.7	88.0	57.1	9.7	6.5	4	3	2	22
		Result 2	87.1	100.0	85.7	42.9	12.9	0.0	3	4	0	24
	RBFN	Result 1	32.3	23.1	80.0	85.7	3.2	64.5	6	1	20	4
		Result 2	77.4	50.0	79.3	14.3	19.4	3.2	1	6	1	23
	JMA	–	86.0	40.0	91.0	33.0	8.0	6.0	–	–	–	–
Aug.	3LP	Result 1	71.0	30.8	100.0	100.0	0.0	29.0	4	0	9	18
		Result 2	80.6	25.0	88.9	25.0	9.7	9.7	1	3	3	24
	RBFN	Result 1	35.5	13.6	88.9	75.0	3.2	61.3	3	1	19	8
		Result 2	83.9	33.3	89.3	25.0	9.7	6.5	1	3	2	25
	JMA	–	90.0	60.0	92.0	33.0	8.0	3.0	–	–	–	–
Sep.	3LP	Result 1	83.3	66.7	87.5	57.1	10.0	6.7	4	3	2	21
		Result 2	70.0	33.3	79.2	28.6	16.7	13.3	2	5	4	19
	RBFN	Result 1	80.0	60.0	84.0	42.9	13.3	6.7	3	4	2	21
		Result 2	80.0	66.7	81.5	28.6	16.7	3.3	2	5	1	22
	JMA	–	83.0	72.0	85.0	49.0	13.0	5.0	–	–	–	–
Oct.	3LP	Result 1	87.1	40.0	96.2	66.7	3.2	9.7	2	1	3	25
		Result 2	87.1	33.3	92.9	33.3	6.5	6.5	1	2	2	26
	RBFN	Result 1	80.6	20.0	92.3	33.3	6.5	12.9	1	2	4	24
		Result 2	74.2	14.3	91.7	33.3	6.5	19.4	1	2	6	22
	JMA	–	92.0	33.0	98.0	63.0	2.0	6.0	–	–	–	–
Nov.	3LP	Result 1	93.3	83.3	95.8	83.3	3.3	3.3	5	1	1	23
		Result 2	90.0	80.0	92.0	66.7	6.7	3.3	4	2	1	23
	RBFN	Result 1	83.3	55.6	95.2	83.3	3.3	13.3	5	1	4	20
		Result 2	86.7	66.7	91.7	66.7	6.7	6.7	4	2	2	22
	JMA	–	90.0	20.0	98.0	50.0	2.0	8.0	–	–	–	–
Dec.	3LP	Result 1	80.6	66.7	84.0	50.0	12.9	6.5	4	4	2	21
		Result 2	74.2	50.0	75.9	12.5	22.6	3.2	1	7	1	22
	RBFN	Result 1	54.8	25.0	73.7	37.5	16.1	29.0	3	5	9	14
		Result 2	58.1	14.3	70.8	12.5	22.6	19.4	1	7	6	17
	JMA	–	90.0	83.0	92.0	79.0	6.0	5.0	–	–	–	–

Table 9
Prediction results for Naha in Jan.–Jun. 2012 (JMA: Okinawa-honto Chunanbu).

Month	Model	Result	Evaluation index (%)						A number of events			
			THR	*HRP*	*HRN*	*CR*	*OR*	*SMR*	*A*	*B*	*C*	*D*
Jan.	3LP	Result 1	67.7	47.4	100.0	100.0	0.0	32.3	9	0	10	12
		Result 2	74.2	53.8	88.9	77.8	6.5	19.4	7	2	6	16
	RBFN	Result 1	58.1	37.5	80.0	66.7	9.7	32.3	6	3	10	12
		Result 2	71.0	50.0	72.4	11.1	25.8	3.2	1	8	1	21
	JMA	–	90.0	70.0	98.0	93.0	1.0	9.0	–	–	–	–
Feb.	3LP	Result 1	69.0	50.0	86.7	77.8	6.9	24.1	7	2	7	13
		Result 2	75.9	62.5	81.0	55.6	13.8	10.3	5	4	3	17
	RBFN	Result 1	65.5	44.4	75.0	44.4	17.2	17.2	4	5	5	15
		Result 2	72.4	100.0	71.4	11.1	27.6	0.0	1	8	0	20
	JMA	–	82.0	46.0	94.0	71.0	5.0	13.0	–	–	–	–
Mar.	3LP	Result 1	74.2	100.0	73.3	11.1	25.8	0.0	1	8	0	22
		Result 2	71.0	50.0	72.4	11.1	25.8	3.2	1	8	1	21
	RBFN	Result 1	71.0	50.0	78.3	44.4	16.1	12.9	4	5	4	18
		Result 2	74.2	100.0	73.3	11.1	25.8	0.0	1	8	0	22
	JMA	–	82.0	40.0	95.0	69.0	4.0	14.0	–	–	–	–
Apr.	3LP	Result 1	66.7	80.0	60.0	50.0	26.7	6.7	8	8	2	12
		Result 2	56.7	100.0	51.9	18.8	43.3	0.0	3	13	0	14
	RBFN	Result 1	70.0	73.3	66.7	68.8	16.7	13.3	11	5	4	10
		Result 2	73.3	90.0	65.0	56.3	23.3	3.3	9	7	1	13
	JMA	–	69.0	46.0	88.0	77.0	6.0	25.0	–	–	–	–
May	3LP	Result 1	74.2	36.4	95.0	80.0	3.2	22.6	4	1	7	19
		Result 2	83.9	50.0	92.0	60.0	6.5	9.7	3	2	3	23
	RBFN	Result 1	74.2	36.4	95.0	80.0	3.2	22.6	4	1	7	19
		Result 2	71.0	30.0	90.5	60.0	6.5	22.6	3	2	7	19
	JMA	–	89.0	60.0	100.0	98.0	0.0	10.0	–	–	–	–
Jun.	3LP	Result 1	63.3	50.0	83.3	81.8	6.7	30.0	9	2	9	10
		Result 2	63.3	50.0	68.2	36.4	23.3	13.3	4	7	4	15
	RBFN	Result 1	66.7	55.6	71.4	45.5	20.0	13.3	5	6	4	15
		Result 2	73.3	80.0	72.0	36.4	23.3	3.3	4	7	1	18
	JMA	–	91.0	78.0	98.0	95.0	1.0	7.0	–	–	–	–

Table 10
Prediction results for Naha in Jul.–Dec. 2012 (JMA: Okinawa-honto Chunanbu).

Month	Model	Result	Evaluation index (%)						A number of events			
			THR	*HRP*	*HRN*	*CR*	*OR*	*SMR*	*A*	*B*	*C*	*D*
Jul.	3LP	Result 1	51.6	35.0	81.8	77.8	6.5	41.9	7	2	13	9
		Result 2	87.1	100.0	84.6	55.6	12.9	0.0	5	4	0	22
	RBFN	Result 1	74.2	54.5	85.0	66.7	9.7	16.1	6	3	5	17
		Result 2	71.0	50.0	72.4	11.1	25.8	3.2	1	8	1	21
	JMA	–	85.0	25.0	94.0	39.0	5.0	10.0	–	–	–	–
Aug.	3LP	Result 1	67.7	64.7	71.4	73.3	12.9	19.4	11	4	6	10
		Result 2	67.7	72.7	65.0	53.3	22.6	9.7	8	7	3	13
	RBFN	Result 1	74.2	81.8	70.0	60.0	19.4	6.5	9	6	2	14
		Result 2	71.0	100.0	64.0	40.0	29.0	0.0	6	9	0	16
	JMA	–	78.0	62.0	87.0	72.0	9.0	14.0	–	–	–	–
Sep.	3LP	Result 1	93.3	100.0	91.7	75.0	6.7	0.0	6	2	0	22
		Result 2	90.0	100.0	88.0	62.5	10.0	0.0	5	3	0	22
	RBFN	Result 1	80.0	66.7	83.3	50.0	13.3	6.7	4	4	2	20
		Result 2	76.7	100.0	75.9	12.5	23.3	0.0	1	7	0	22
	JMA	–	77.0	42.0	90.0	61.0	7.0	16.0	–	–	–	–
Oct.	3LP	Result 1	87.1	71.4	91.7	71.4	6.5	6.5	5	2	2	22
		Result 2	83.9	100.0	82.8	28.6	16.1	0.0	2	5	0	24
	RBFN	Result 1	90.3	100.0	88.9	57.1	9.7	0.0	4	3	0	24
		Result 2	83.9	66.7	88.0	57.1	9.7	6.5	4	3	2	22
	JMA	–	97.0	100.0	97.0	69.0	3.0	0.0	–	–	–	–
Nov.	3LP	Result 1	86.7	100.0	85.7	33.3	13.3	0.0	2	4	0	24
		Result 2	83.3	100.0	82.8	16.7	16.7	0.0	1	5	0	24
	RBFN	Result 1	83.3	100.0	82.8	16.7	16.7	0.0	1	5	0	24
		Result 2	76.7	33.3	81.5	16.7	16.7	6.7	1	5	2	22
	JMA	–	97.0	82.0	100.0	100.0	0.0	3.0	–	–	–	–
Dec.	3LP	Result 1	83.9	62.5	91.3	71.4	6.5	9.7	5	2	3	21
		Result 2	90.3	100.0	88.9	57.1	9.7	0.0	4	3	0	24
	RBFN	Result 1	83.9	66.7	88.0	57.1	9.7	6.5	4	3	2	22
		Result 2	77.4	50.0	81.5	28.6	16.1	6.5	2	5	2	22
	JMA	–	91.0	62.0	99.0	95.0	1.0	9.0	–	–	–	–

Table 11
Total prediction results in 2012.

Obs. point	Model	Result	Evaluation index (%)						A number of events			
			THR	*HRP*	*HRN*	*CR*	*OR*	*SMR*	*A*	*B*	*C*	*D*
Sapporo	3LP	Result 1	76.8	61.7	88.7	81.3	6.3	16.9	100	23	62	181
		Result 2	80.1	74.0	82.4	62.6	12.6	7.4	77	46	27	216
	RBFN	Result 1	62.6	46.1	78.2	66.7	11.2	26.2	82	41	96	147
		Result 2	68.3	55.4	71.1	29.3	23.8	7.9	36	87	29	214
	JMA	–	80.0	55.0	92.0	76.0	5.0	15.0	–	–	–	–
Matsuyama	3LP	Result 1	83.2	62.6	90.1	67.9	7.4	9.3	57	27	34	246
		Result 2	82.4	70.0	84.4	41.7	13.5	4.1	35	49	15	265
	RBFN	Result 1	68.4	38.3	85.7	60.7	9.1	22.5	51	33	82	198
		Result 2	77.7	53.1	81.6	31.0	15.9	6.3	26	58	23	257
	JMA	–	90.0	65.0	94.0	69.0	5.0	6.0	–	–	–	–
Naha	3LP	Result 1	73.8	55.6	84.1	66.7	10.1	16.1	74	37	59	196
		Result 2	77.3	70.6	78.9	43.2	17.2	5.5	48	63	20	235
	RBFN	Result 1	74.3	57.9	81.1	55.9	13.4	12.3	62	49	45	210
		Result 2	74.3	66.7	75.6	30.6	21.0	4.6	34	77	17	238
	JMA	–	86.0	57.0	95.0	80.0	4.0	11.0	–	–	–	–

ing. Thus, the training condition was worse than that of the previous experiment in Section 4.3. The RBFN NNs were trained at 101 of the standard deviation, as shown in Eq. (25).

Table 12 shows the experimental results. From the result of Section 4.3, we chosen the result of NNs of the largest A at each observation point. In the experimental results, 3LP outperformed RBFN without the result of Hikone as well as the results of the experiments in Section 4.3. It was thus that precipitation over Japan can be predicted by the proposed method; however, the results of 3LP were worse than those of JMA in total.

5. Heavy rainfall in Tokyo

In this section, we describe experiments to predict heavy rainfall in summer afternoons in Tokyo, specifically, Jun.–Sept. 2011 and 2012.

5.1. Conditions

In technical terms of the JMA, cloudburst means several hundreds of millimeters of heavy rainfall for several hours, and "unexpected local heavy rain (guerrilla rainstorm)" represents heavy rainfall that occurs suddenly with a volume of 50–100 mm/h within minutes in a small area; however, its range and total amount have not been defined clearly in the academic literature [51]. If the condition of the objective rainfall is too narrow, the training data of the NNs was found to be lacking. Therefore, the objective sudden heavy rainfall was defined as rainfall satisfying the following conditions:

The conditions for heavy rainfall

(i) Rainfall above 10 mm/h in the afternoon (12:00–24:00 JST)
(ii) There was no rainfall above 0.5 mm/h between 9:00 and 12:00 JST

5.2. Experiment

When collecting data relating to local heavy rainfall in the afternoons during the summer in Tokyo, research on "Nerima Gouu (cloudburst) in Tokyo on Jul. 21, 1999" was used as reference. Mikami reported that this occurrence is affected by the heat island phenomenon, which occurs before it, and the updraft due to the convergence of wind from nearby areas—Tokyo Bay (Tokyo), Sagmi Bay (Kanagawa), and Kashima-nada (Chiba)— [43]. Therefore, data on wind direction, velocity, atmospheric pressure, and temperature of the observation points around Tokyo—Edogawa-rinkai (Tokyo),

Fig. 8. Observation points around Tokyo (the map image from CraftMAP [50]).

Ebina (Kanagawa), and Abiko (Chiba) (Fig. 8)—at 9:00, 10:00, 11:00, and 12:00 JST were added to the training data, and the data in Table 2 and wind direction (Table 3) data of Tokyo at 9:00, 10:00, 11:00, and 12:00 JST, were used as the inputs to the teaching signals (total number: 84). The morning data close to the afternoon were used as training data because the predicted rainfall was the consequence of rapid climate change. In training the NNs, the output of the teaching signals was defined as "1 when the heavy rainfall condition was satisfied" and "0 when the heavy rainfall condition was not satisfied." In the prediction, a result was defined as "rainfall when the output of NNs $\geq 0.5''$ and "non-rainfall when the output of NNs $< 0.5''$. The rainfall in Aug. and Sept. of 2011 was predicted by data from the same months in 2000–2010, and the rainfall in Jun. and Sept. of 2012 was predicted by data from the same months in 2000–2011. In the experiments, 30 of the 3LP NN were trained while changing each of the initial weights, and 101 of the RBFN NNs were trained while changing the standard deviation as in Eq. (25).

Table 13 shows the top five results for heavy rainfall prediction. If five patterns of results for each experiment were not obtained, the result was represented as "–". Heavy rainfall in Tokyo was predicted with $CR = 100\%$ and $OR = 0\%$ without result 1 from RBFN in Sept. 2011, and is important for disaster prevention. However, *HRP* was very low, namely, "the boy who cried wolf." Moreover, the result of 3LP was better than that of RBFN in general, and there was a

Table 12
Averages prediction results for 2012.

Obs. point	Model	Evaluation index (%)						A number of events			
		THR	*HRP*	*HRN*	*CR*	*OR*	*SMR*	*A*	*B*	*C*	*D*
Wakkanai (Souya)	3LP	83.3	64.9	88.0	57.8	9.6	7.1	48	35	26	257
	RBFN	75.1	45.2	84.0	45.8	12.3	12.6	38	45	46	237
	JMA	80.0	55.0	92.0	76.0	5.0	15.0	–	–	–	–
Asahikawa (Kamikawa)	3LP	78.4	51.6	87.8	59.8	9.0	12.6	49	33	46	237
	RBFN	71.0	39.1	84.7	52.4	10.7	18.4	43	39	67	216
	JMA	81.0	58.0	92.0	76.0	6.0	13.0	–	–	–	–
Aomori (Aomori Tsugaru)	3LP	78.1	50.9	90.8	72.0	6.3	15.6	59	23	57	227
	RBFN	74.9	44.6	85.0	50.0	11.2	13.9	41	41	51	233
	JMA	81.0	58.0	95.0	86.0	3.0	15.0	–	–	–	–
Akita (Akita Engan)	3LP	81.6	61.0	87.6	58.8	9.6	8.8	50	35	32	248
	RBFN	73.2	43.7	84.7	52.9	11.0	15.9	45	40	58	222
	JMA	81.0	61.0	94.0	86.0	4.0	15.0	–	–	–	–
Mito (Ibaragi Hokubu)	3LP	85.5	52.6	91.6	53.6	7.1	7.4	30	26	27	282
	RBFN	79.5	37.0	90.1	48.2	7.9	12.6	27	29	46	263
	JMA	90.0	65.0	97.0	86.0	2.0	7.0	–	–	–	–
Utsunomiya (Tochigi Nanbu)	3LP	86.6	58.9	91.6	55.9	7.1	6.3	33	26	23	284
	RBFN	78.7	38.0	89.9	50.8	7.9	13.4	30	29	49	258
	JMA	90.0	64.0	97.0	84.0	3.0	8.0	–	–	–	–
Shizuoka (Shizuoka Chubu)	3LP	87.7	63.8	91.2	51.7	7.7	4.7	30	28	17	290
	RBFN	69.9	25.9	88.3	48.3	8.2	21.9	28	30	80	227
	JMA	92.0	78.0	95.0	78.0	4.0	4.0	–	–	–	–
Nagoya (Aichi Seibu)	3LP	90.4	60.0	95.2	66.7	4.1	5.5	30	15	20	300
	RBFN	84.1	40.3	94.0	60.0	4.9	11.0	27	18	40	280
	JMA	92.0	66.0	98.0	91.0	1.0	6.0	–	–	–	–
Niigata (Niigata Kaetsu)	3LP	82.7	62.5	89.1	64.7	8.2	9.1	55	30	33	246
	RBFN	73.1	43.6	84.4	51.8	11.3	15.7	44	41	57	222
	JMA	87.0	75.0	94.0	86.0	4.0	5.0	–	–	–	–
Toyama (Toyama Toubu)	3LP	77.3	57.4	88.2	72.5	7.7	15.0	74	28	55	209
	RBFN	74.6	53.5	85.8	66.7	9.3	16.1	68	34	59	205
	JMA	86.0	73.0	94.0	88.0	4.0	10.0	–	–	–	–
Hikone (Shiga Hokubu)	3LP	84.1	54.2	89.9	50.8	8.5	7.4	32	31	27	275
	RBFN	76.4	38.6	90.9	61.9	6.6	17.0	39	24	62	240
	JMA	85.0	63.0	94.0	84.0	4.0	11.0	–	–	–	–
Okayama (Okayama Nanbu)	3LP	89.9	50.0	95.6	62.2	3.8	6.3	23	14	23	306
	RBFN	87.7	42.0	94.9	56.8	4.4	7.9	21	16	29	300
	JMA	94.0	72.0	97.0	75.0	3.0	3.0	–	–	–	–
Shimonoseki (Yamaguchi Seibu)	3LP	81.4	36.8	93.1	58.3	5.5	13.1	28	20	48	270
	RBFN	82.2	36.5	91.7	47.9	6.8	10.9	23	25	40	278
	JMA	91.0	64.0	97.0	82.0	2.0	6.0	–	–	–	–
Tokushima (Tokushima Hokubu)	3LP	89.5	56.8	94.0	56.8	5.2	5.2	25	19	19	300
	RBFN	79.9	26.2	90.7	36.4	7.7	12.4	16	28	45	274
	JMA	85.0	51.0	93.0	65.0	5.0	10.0	–	–	–	–
Miyazaki (Miyazaki Nanbu–heiyabu)	3LP	88.8	71.8	93.4	74.7	5.2	6.0	56	19	22	268
	RBFN	79.2	49.4	87.7	53.3	9.6	11.2	40	35	41	249
	JMA	89.0	74.0	93.0	76.0	5.0	6.0	–	–	–	–
Naha (Okinawa–honto Chunanbu)	3LP	77.9	41.1	89.9	56.9	7.7	14.5	37	28	53	248
	RBFN	80.9	46.7	89.7	53.8	8.2	10.9	35	30	40	261
	JMA	86.0	57.0	95.0	80.0	4.0	11.0	–	–	–	–

trade-off relationship between *A* and *D* in the result of 3LP in Aug. and Sept., 2011, as well as in the experiment in Section 4.3.

6. Conclusion and future work

This paper proposed local rainfall prediction based on NNs using meteorological data obtained from the website of the JMA. The effectiveness of JMA data for local rainfall prediction in Japan was confirmed. The precipitation of Sapporo, Matsuyama, and Naha was first predicted, followed by precipitation at 16 points over Japan. The prediction results were compared with the JMA's results. We observed that the proposed method was outperformed by JMA's prediction. Finally, heavy rainfall in summer afternoons in Tokyo was predicted, and the results suggested the possibility of the prediction of unexpected local heavy rainfall as "guerrilla rainstorms". From these results, it can be shown that 3LP is better than RBFN for the precipitation prediction problem, and there is a trade-off relationship between the hit rate of precipitation *A* and non-precipitation *D*. In this study, the number of trained NNs was 20 or 30 for 3LP and 101 for RBFN in the experiments. We can conclude that NNs are better trained and more accurate for prediction if these numbers are increased in value. Furthermore, better machine-learning models need to be investigated to improve prediction performance (e.g., support vector machines and random forest). Furthermore, an investigation is needed into the method used to choose meteorological data because suitable data can be

Table 13
Prediction results of heavy rainfall in Tokyo in 2011 and 2012.

Month	Model	Result	Evaluation indices (%)						A number of events			
			THR	*HRP*	*HRN*	*CR*	*OR*	*SMR*	*A*	*B*	*C*	*D*
Aug. 2011	3LP	Result 1	80.6	33.3	100.0	100.0	0.0	19.4	3	0	6	22
		Result 2	77.4	30.0	100.0	100.0	0.0	22.6	3	0	7	21
		Result 3	80.6	28.6	95.8	66.7	3.2	16.1	2	1	5	23
		Result 4	77.4	25.0	95.7	66.7	3.2	19.4	2	1	6	22
		Result 5	74.2	22.2	95.5	66.7	3.2	22.6	2	1	7	21
	RBFN	Result 1	67.7	23.1	100.0	100.0	0.0	32.3	3	0	10	18
		Result 2	64.5	21.4	100.0	100.0	0.0	35.5	3	0	11	17
		Result 3	61.3	20.0	100.0	100.0	0.0	38.7	3	0	12	16
		Result 4	58.1	18.8	100.0	100.0	0.0	41.9	3	0	13	15
		Result 5	51.6	16.7	100.0	100.0	0.0	48.4	3	0	15	13
Sep. 2011	3LP	Result 1	79.3	25.0	100.0	100.0	0.0	20.7	2	0	6	21
		Result 2	27.6	8.7	100.0	100.0	0.0	72.4	2	0	21	6
		Result 3	82.8	20.0	95.8	50.0	3.4	13.8	1	1	4	23
		Result 4	79.3	16.7	95.7	50.0	3.4	17.2	1	1	5	22
		Result 5	75.9	14.3	95.5	50.0	3.4	20.7	1	1	6	21
	RBFN	Result 1	51.7	7.1	93.3	50.0	3.4	44.8	1	1	13	14
		Result 2	48.3	6.7	92.9	50.0	3.4	48.3	1	1	14	13
		Result 3	44.8	6.3	92.3	50.0	3.4	51.7	1	1	15	12
		Result 4	–	–	–	–	–	–	–	–	–	–
		Result 5	–	–	–	–	–	–	–	–	–	–
Jun. 2012	3LP	Result 1	90.0	25.0	100.0	100.0	0.0	10.0	1	0	3	26
		Result 2	83.3	16.7	100.0	100.0	0.0	16.7	1	0	5	24
		Result 3	76.7	12.5	100.0	100.0	0.0	23.3	1	0	7	22
		Result 4	73.3	11.1	100.0	100.0	0.0	26.7	1	0	8	21
		Result 5	70.0	10.0	100.0	100.0	0.0	30.0	1	0	9	20
	RBFN	Result 1	53.3	6.7	100.0	100.0	0.0	46.7	1	0	14	15
		Result 2	46.7	5.9	100.0	100.0	0.0	53.3	1	0	16	13
		Result 3	43.3	5.6	100.0	100.0	0.0	56.7	1	0	17	12
		Result 4	36.7	5.0	100.0	100.0	0.0	63.3	1	0	19	10
		Result 5	30.0	4.5	100.0	100.0	0.0	70.0	1	0	21	8
Sep. 2012	3LP	Result 1	75.9	22.2	100.0	100.0	0.0	24.1	2	0	7	20
		Result 2	72.4	20.0	100.0	100.0	0.0	27.6	2	0	8	19
		Result 3	62.1	15.4	100.0	100.0	0.0	37.9	2	0	11	16
		Result 4	55.2	13.3	100.0	100.0	0.0	44.8	2	0	13	14
		Result 5	44.8	11.1	100.0	100.0	0.0	55.2	2	0	16	11
	RBFN	Result 1	69.0	18.2	100.0	100.0	0.0	31.0	2	0	9	18
		Result 2	65.5	16.7	100.0	100.0	0.0	34.5	2	0	10	17
		Result 3	62.1	15.4	100.0	100.0	0.0	37.9	2	0	11	16
		Result 4	58.6	14.3	100.0	100.0	0.0	41.4	2	0	12	15
		Result 5	55.2	13.3	100.0	100.0	0.0	44.8	2	0	13	14

different among prediction points due to the difference in the effect of conditions, such as altitude, ocean current, airflow, etc. The accurate prediction of precipitation, namely, larger *A*, is most important from the point of view of disaster prevention; however, it can cause a situation of the "the boy who cried wolf." Therefore, the compatibility of both the prediction of precipitation and non-precipitation persists as an issue for future research.

In future work, we plan to predict local precipitation based on local data obtained from a meteorological data logger installed at the NIT, Niihama College (Ehime, Japan). Moreover, a system to share data among users (such as individuals, schools, universities, companies, etc.) via the Internet will be developed. If meteorological data around the prediction point can be shared with users, the accuracy of prediction can be improved. Moreover, data collection and selection methods from big data using deep-learning technology will be developed to improve the developed system.

Acknowledgments

This work was supported by the National Institute of Technology, Niihama College, Japan, and Southern Cross University, Australia. We are grateful to Prof. Koichi Suzuki, Prof. Shuji Sakohara, Prof. Mikio Deguchi, and Prof. Scott T. Smith for their support.

References

[1] JMA, JMA numerical weather prediction, http://www.jma.go.jp/jma/jma-eng/jma-center/nwp/nwp-top.htm (16.07.15).
[2] B. Norio, K. Fumio, O. Seiichi, Foundations of Neural Networks and Applications, Kyoritsu Shuppan, 1994 (in Japanese).
[3] G.P. Liu, Nonlinear Identification and Control: A NEURAL network Approach, Springer Science & Business Media, 2012.
[4] B. Norio, T. Masahiro, Y. Yasunari, M. Yasue, H. Hisashi, Foundations of Soft Computing and Applications, Kyoritsu Shuppan, Tokyo, Japan, 2012 (in Japanese). https://books.google.com.au/books?id=AMfBuAAACAAJ.
[5] A.J. Maren, C.T. Harston, R.M. Pap, Handbook of Neural Computing Applications, Academic Press, 2014.
[6] D.R. Nayak, A. Mahapatra, P. Mishra, A survey on rainfall prediction using artificial neural network, Int. J. Comput. Appl. 72 (16) (2013).
[7] M.A. Ahmadi, R. Soleimani, M. Lee, T. Kashiwao, A. Bahadori, Determination of oil well production performance using artificial neural network (ANN) linked to the particle swarm optimization (PSO) tool, Petroleum 1 (2) (2015) 118–132.
[8] A. Tatar, S. Naseri, M. Bahadori, J. Rozyn, M. Lee, T. Kashiwao, A. Bahadori, Evaluation of different artificial intelligent models to predict reservoir formation water density, Pet. Sci. Technol. 33 (20) (2015) 1749–1756.
[9] M. Ahmadi, T. Kashiwao, A. Bahadori, Prediction of oil production rate using vapor-extraction technique in heavy oil recovery operations, Pet. Sci. Technol. 33 (20) (2015) 1764–1769.
[10] A. Tatar, A. Shokrollahi, M. Lee, T. Kashiwao, A. Bahadori, Prediction of supercritical CO_2/brine relative permeability in sedimentary basins during carbon dioxide sequestration, Greenh. Gases Sci. Technol. 5 (6) (2015) 756–771.
[11] S. Naseri, A. Tatar, M. Bahadori, J. Rozyn, T. Kashiwao, A. Bahadori, Application of radial basis function neural network for prediction of titration-based asphaltene precipitation, Pet. Sci. Technol. 33 (23-24) (2015) 1875–1882.

[12] E. Soroush, M. Mesbah, A. Shokrollahi, J. Rozyn, M. Lee, T. Kashiwao, A. Bahadori, Evolving a robust modeling tool for prediction of natural gas hydrate formation conditions, J. Unconv. Oil Gas Resour. 12 (2015) 45–55.
[13] M. Ahmadi, T. Kashiwao, J. Rozyn, A. Bahadori, Accurate prediction of properties of carbon dioxide for carbon capture and sequestration operations, Pet. Sci. Technol. 34 (1) (2016) 97–103.
[14] Z. Ahmad, J. Zhang, T. Kashiwao, A. Bahadori, Prediction of absorption and stripping factors in natural gas processing industries using feedforward artificial neural network, Pet. Sci. Technol. 34 (2) (2016) 105–113.
[15] A. Bahadori, A. Baghban, M. Bahadori, T. Kashiwao, M.V. Ayouri, Estimation of emission of hydrocarbons and filling losses in storage containers using intelligent models, Pet. Sci. Technol. 34 (2) (2016) 145–152.
[16] M. Ahmadi, T. Kashiwao, M. Bahadori, A. Bahadori, Estimation of water-hydrocarbon mutual solubility in gas processing operations using an intelligent model, Pet. Sci. Technol. 34 (4) (2016) 328–334.
[17] A. Tatar, A. Najafi-Marghmaleki, A. Barati-Harooni, A. Gholami, H. Ansari, M. Bahadori, T. Kashiwao, M. Lee, A. Bahadori, Implementing radial basis function neural networks for prediction of saturation pressure of crude oils, Pet. Sci. Technol. 34 (5) (2016) 454–463.
[18] J.S. Amin, A. Bahadori, T. Kashiwao, Z. Ahmad, B.A. Souraki, S. Rafiee, A new empirical correlation for prediction of carbon dioxide separation from different gas mixtures, Pet. Sci. Technol. 34 (6) (2016) 562–569.
[19] A. Baghban, M. Bahadori, T. Kashiwao, A. Bahadori, Modelling of gas to hydrate conversion for promoting CO_2 capture processes in the oil and gas industry, Pet. Sci. Technol. 34 (7) (2016) 642–651.
[20] J.S. Amin, M. Bahadori, M. Lee, T. Kashiwao, A. Bahadori, S. Rafiee, B.H. Nia, Prediction of carbon dioxide separation from gas mixtures in petroleum industries using the Levenberg–Marquardt algorithm, Pet. Sci. Technol. 34 (8) (2016) 703–711.
[21] S. Lee, S. Cho, P.M. Wong, Rainfall prediction using artificial neural networks, J. Geogr. Inf. Decis. Anal. 2 (2) (1998) 233–242.
[22] K. Koizumi, An objective method to modify numerical model forecasts with newly given weather data using an artificial neural network, Weather Forecast. 14 (1) (1999) 109–118.
[23] K. Koizumi, M. Hirasawa, A neural-network structure suitable for precipitation amount forecast, TENKI 48 (12) (2001) 885–892 (in Japanese).
[24] K.C. Luk, J.E. Ball, A. Sharma, An application of artificial neural networks for rainfall forecasting, Math. Comput. Model. 33 (6) (2001) 683–693.
[25] S. Ito, Y. Mitsukura, M. Fukumi, N. Akamatsu, Neuro rainfall forecast with data mining by real-coded genetical preprocessing, IEEJ Trans. Electron. Inf. Syst. 123 (2003) 817–822 (in Japanese).
[26] N.Q. Hung, M.S. Babel, S. Weesakul, N. Tripathi, An artificial neural network model for rainfall forecasting in Bangkok, Thailand, Hydrol. Earth Syst. Sci. 13 (8) (2009) 1413–1425.
[27] K. Abhishek, A. Kumar, R. Ranjan, S. Kumar, A rainfall prediction model using artificial neural network, in: Control and System Graduate Research Colloquium (ICSGRC), 2012 IEEE, IEEE, 2012, pp. 82–87.
[28] J. Abbot, J. Marohasy, Application of artificial neural networks to rainfall forecasting in Queensland, Australia, Adv. Atmos. Sci. 29 (4) (2012) 717–730.
[29] P. Singh, B. Borah, Indian summer monsoon rainfall prediction using artificial neural network, Stoch. Environ. Res. Risk Assess. 27 (7) (2013) 1585–1599.
[30] A. Alqudah, V. Chandrasekar, M. Le, Investigating rainfall estimation from radar measurements using neural networks, Nat. Hazards Earth Syst. Sci. 13 (3) (2013) 535–544.
[31] S. Koumura, Y. Matsuda, Y. Sekine, Y. Shidama, H. Yamaura, Local weather prediction system by neural networks. IEICE technical report, Neurocomputing 94 (182) (1994) 25–32 (in Japanese).
[32] C. Dawson, R. Wilby, Hydrological modelling using artificial neural networks, Prog. Phys. Geogr. 25 (1) (2001) 80–108.
[33] Y.B. Dibike, D.P. Solomatine, River flow forecasting using artificial neural networks, Phys. Chem. Earth Part B: Hydrol. Oceans Atmos. 26 (1) (2001) 1–7.
[34] H.K. Cigizoglu, M. Alp, Rainfall-runoff modelling using three neural network methods, in: Artificial Intelligence and Soft Computing-ICAISC 2004, Springer, 2004, pp. 166–171.
[35] A. Senthil Kumar, K. Sudheer, S. Jain, P. Agarwal, Rainfall-runoff modelling using artificial neural networks: comparison of network types, Hydrol. Process. 19 (6) (2005) 1277–1291.
[36] M. Shoaib, A.Y. Shamseldin, B.W. Melville, Comparative study of different wavelet based neural network models for rainfall-runoff modeling, J. Hydrol. 515 (2014) 47–58.
[37] M. Zare, H.R. Pourghasemi, M. Vafakhah, B. Pradhan, Landslide susceptibility mapping at VAZ watershed (Iran) using an artificial neural network model: a comparison between multilayer perceptron (MLP) and radial basic function (RBF) algorithms, Arab. J. Geosci. 6 (8) (2013) 2873–2888.
[38] T. Kashiwao, S. Ando, K. Ikeda, T. Shimomura, Neural network-based local prediction of rainfall using meteorological data on the internet), Trans. Inst. Syst., Control Inf. Eng. 28 (3) (2015) 123–125 (in Japanese).
[39] J. Manyika, M. Chui, B. Brown, J. Bughin, R. Dobbs, C. Roxburgh, A.H. Byers, Big data: the next frontier for innovation, competition, and productivity, 2011.
[40] A. McAfee, E. Brynjolfsson, T.H. Davenport, D. Patil, D. Barton, Big data, the management revolution, Harv. Bus. Rev. 90 (10) (2012) 61–67.
[41] Y.-G. Jung, H. Jin, Experimental comparisons of neural networks and logistic regression models for heart disease prediction, Information 16 (2) (2013).
[42] B.C. Pijanowski, A. Tayyebi, J. Doucette, B.K. Pekin, D. Braun, J. Plourde, A big data urban growth simulation at a national scale: configuring the GIS and neural network based land transformation model to run in a high performance computing (HPC) environment, Environ. Model. Softw. 51 (2014) 250–268.
[43] T. Mikami, H. Yamamoto, H. Ando, H. Yokoyama, T. Yamaguchi, M. Ichino, Y. Akiyama, K. Ishii, Climatological study on the summer intensive heavy rainfall in Tokyo, Annu. Rep. Tokyo Metrop. Res. Inst. Environ. Protect. 2005 (2005) 33–42 (in Japanese).
[44] T. Yamanaka, R. Ooka, Analysis of urban effect on local heavy rainfall in Tokyo using mesoscale model, The seventh International Conference on Urban Climate (2009).
[45] T. Kawabata, T. Kuroda, H. Seko, K. Saito, A cloud-resolving 4DVAR assimilation experiment for a local heavy rainfall event in the Tokyo metropolitan area, Mon. Weather Rev. 139 (6) (2011) 1911–1931.
[46] K. Souma, K. Sunada, T. Suetsugi, K. Tanaka, Use of ensemble simulations to evaluate the urban effect on a localized heavy rainfall event in Tokyo, Japan, J. Hydroenviron. Res. 7 (4) (2013) 228–235.
[47] JMA, Meteorological observation data, http://www.jma.go.jp/jma/menu/obsmenu.html (in Japanese) (1 Jul. 2015).
[48] D. Erhan, Y. Bengio, A. Courville, P.-A. Manzagol, P. Vincent, S. Bengio, Why does unsupervised pre-training help deep learning? J. Mach. Learn. Res. 11 (2010) 625–660.
[49] JMA, Results of accuracy verification of a weather forecast, http://www.data.jma.go.jp/fcd/yoho/kensho/yohohyoka_top.html (in Japanese) (16.07.15).
[50] CraftMAP, http://www.craftmap.box-i.net/ (in Japanese) (01.07.15).
[51] JMA, Precipitation, http://www.jma.go.jp/jma/kishou/know/yougo_hp/kousui.html (in Japanese) (16.07.15).